Int. J. Advanced Design and Manufacturing Technology, 2023, Vol. 16, No. 4, pp. 69-77

DOI: 10.30486/admt.2024.1994136.1418 ISSN: 2252-0406 https://admt.isfahan.iau.ir

Effect of Post-Weld Heat Treatment on Microstructure and Mechanical Properties of AA7075 Welds

Alireza Jalil, Nasrollah Bani Mostafa Arab *
Faculty of Mechanical Engineering,
Shahid Rajaee Teacher Training University, Tehran, Iran
E-mail: ar.jalil@sru.ac.ir, n.arab@sru.ac.ir
*Corresponding author

Malek Naderi
Department of Materials and Metallurgical Engineering,
Amirkabir University of Technology, Tehran, Iran
E-mail: mnaderi@aut.ac.ir

Yaghoub Dadgar Asl
Department of Mechanical Engineering,
Technical and Vocational University, Tehran, Iran
E-mail: ydadgar@tvu.ac.ir

Received: 17 August 2023, Revised: 28 November 2023, Accepted: 30 November 2023

Abstract: The attractive mechanical properties of 7075 alloy, such as its high strength-to-weight ratio and fracture toughness, have received special attention in the automotive and aerospace industries. However, welding as a fabrication process has a detrimental effect on this alloy's properties which affects its mechanical performance. In this work, to compensate for the loss in mechanical properties caused by welding, proper heat treatment operations are adopted. To this end, 1.5 mm AA7075 sheets were first preheated and butt welded using the gas tungsten arc welding process. The welded sample was solution heat treated, quenched, and then artificially aged. Microhardness tests showed an increase of hardness in all zones of the aged specimen compared to those of the original welded blank before heat treatment. A maximum microhardness value of 180 HV was recorded in the heat-affected zone of the aged specimen. In addition, elongation at break, and strength (yield, tensile, and fracture) of the original welded blank increased by about 50% after the artificial aging operation.

Keywords: AA7075, Mechanical Properties, Post-Weld Heat Treatment, TIG Welding

Biographical notes: Alireza Jalil is a PhD student in the field of manufacturing engineering at Shahid Rajaee Teacher Training University, Tehran, Iran. He received his MSc from Shahid Rajaee Teacher Training University in 2014. **Nasrollah Bani Mostafa Arab** is an Associate professor of Mechanical Engineering at Shahid Rajaee Teacher Training University, Iran. He received his PhD from IIT Delhi, India, in 1993. **Malek Naderi** is a Professor in the Department of Mining and Metallurgical Engineering, at Amirkabir University of Technology, Tehran, Iran. He received his PhD from RWTH Aachen University in Germany, in 2007. **Yaqoub Dadgar Asl** is an assistant professor in the Department of Mechanical Engineering at Technical and Vocational University, Iran. He received his PostDoc in mechanical engineering from Pusan National University, South Korea, in 2019.

Research paper

1 INTRODUCTION

The environmental concerns and requirements of greenhouse gas emissions have led transportation industries to lightweight products. Aluminum alloys as a subset of lightweight materials are abundantly used in automotive and aircraft structures due to their low density, high strength-to-weight ratio, and good corrosion resistance [1]. Among aluminum alloys, the AA7075 alloy with precipitates of Mg_2Zn and Al_2CuMg phases presents the strength and stiffness required for the body in white (BIW) in aerospace and automotive industries [2]. This alloy is a precipitate-strengthened alloy with the additions of zinc, magnesium, and copper alloying elements.

The Solution Heat Treatment (SHT) process on 7075 Al alloy as a heat-treatable Al−Zn−Mg−Cu alloy, influences the content and distribution of the coarse secondary phases and the evolution of the microstructure, thus leading to a change in the mechanical properties of the alloy. The distribution and size of precipitates mainly depend on the SHT process. Hence, a suitable SHT condition is important to gain proper mechanical properties. It has also been reported that aging is the most preferred method to improve the hardness and strength of AA7075 [3]. During aging, precipitation occurs in a super-saturated aluminum solid solution, and then the alloy's hardness and strength increase [4]. Aging is the precipitation strengthening that provides by far the strongest contribution to the strength of aged Al-Zn-Mg-Cu alloys.

The precipitation mechanism of aging or precipitate hardening in most commercially 7xxx alloys such as AA7075 is α → Guinier Preston (GP) zones → η′ → η. Here α represents supersaturated solid solution (SSS) and is obtained by rapid cooling to room temperature after taking it into solution. The η phase is the equilibrium phase with a hexagonal structure containing Al, Zn, Mg, and Cu, which can be considered to be based on a solid solution of $MgZn_2$ with AlCuMg components (i.e., Mg $(Zn, Al, Mg)_2$ or Mg $(Zn_2, AlMg)$). However, η′ phase (fine precipitates of Zn and Mg-rich metastable $MgZn_2$ phase) is a metastable hexagonal phase. GP zones can form as progenitors of the metastable η′ phase. The age-strengthening factor of AA7075 is more related to fine-scale precipitation of the metastable η′ phase and has a very important role in the mechanical properties of the 7075 alloy. η' phase occurs after aging at 120 ◦C for 4 h, and phases form after 24 h aging time. The size, shape, concentration, and distribution of precipitates are effective parameters for the mechanical properties of this alloy [5-8]. XU et al. [9] observed that $MgZn_2$ particles completely dissolved at a heat treatment of 475°C for 5 minutes. The Al_2CuMg phase gradually disappeared and finally dissolved into the matrix completely at 490 °C, and the Al_7Cu_2Fe phase exhibited no change during the SHT [10].

Welding is one of the most common joining methods for aluminum alloys and tungsten inert gas (TIG) is one of the most used welding processes [11]. As an efficient metal joining process, the welding process makes the joint's strength equal to or sometimes greater than the strength of the base metal and has been widely used in almost all branches of industry [12-13]. In spite of advantages, welding Al-Zn-Mg-Cu aluminum alloys is difficult because of the weld metal zone's porosity, slag inclusion, and cracks. Welding as a production process has a negative impact on the mechanical properties of AA7075 alloy which significantly decreases these properties compared to the base material [14]. Significant strength reduction after the gas tungsten arc welding process (GTAW) and thus considerably lower hardness in the fusion zone (FZ) and heat affected zones (HAZs) are the result of significant precipitate dissolution and coarsening of heat-treatable alloys undergoing high welding temperatures [15]. AA 7075 alloy also exhibits hot cracking and porosity defects via fusion-based additive manufacturing methods. Appropriate post-weld heat treatment can be used to overcome the loss in mechanical properties caused by welding.

To improve the mechanical performance of welded joints, an appropriate post-weld heat treatment is required for the 7xxx aluminum alloy joints [8]. The post-weld heat treatment has shown a practical option to recover the strength of the joints by modifying the graining and distribution of the secondary strengthening particles, therefore it can be an effective method of improving the mechanical properties of welded joints [8], [11].

Liu Xiao et al. [16] carried out TIG butt welding of 7075 aluminum alloy by a self-made 7075 wire before and after heat treatment. They reported that after heat treatment, the mechanical properties of the joint greatly improved. The maximum elongation and tensile strength reached 16.9% and 94% of the base metal (BM). Before heat treatment, η($MgZn_2$), S($CuMgAl_2$), T(AlZnMgCu), and other precipitates distributed continuously at the grain boundary, reduced the mechanical properties of the joint and weakened the influence of grain size. After heat treatment, most of the precipitated phases dissolved into the matrix, and the grain size became the main factor affecting the mechanical properties of the joint. Using TIG AA7075 welding, Tusk et al. [17] found the formation of hot cracks in welded joints and studied the effect of heat treatment and cooling rate on mechanical and microstructural properties. The filler metal type has an important effect on the properties of the welded joint. Welding with dissimilar filler materials aims to dilute the crack-sensitive BM with less crack-sensitive filler material. By diluting the melting zone with dissimilar filler, the concentration of alloy elements of AA7075

decreases. This leads to a decrease in weld strength and an increase in the likelihood of liquation cracking [18]. Kou et al. [19] found aluminum filler alloys such as ER5356 cause the melting zone to solidify earlier than the partially melted zone abutting the melt pool (pure AA7075), creating tension towards the center of the melt pool leading to liquation cracks.

For some authors, the loss of hardness in the boundary between the BM and the HAZ is the major reason for the failure in aluminum alloys. The hardening phase dissolution operation in the matrix during the welding causes a reduction in the mechanical properties of the HAZ. Also, the increased grain size near the molten pool applies greater softening [20]. One way to control solidification cracking is to correct the FZ grain structure with fine-grained coaxial grains. Coarse columnar grains are more prone to solidification cracks than fine coaxial grains while fine-grained coaxial grains deform more easily with contractile strains [21].

Few studies have reported GTAW welding of AA7075 with features of SHT and aging on the mechanical properties of the welded joints. In the present study, preheated 1.5 mm thick AA7075 sheets were initially butt joined using the GTAW welding process. The welded sample was subjected to SHT, then rapidly quenched in a cooling die to form a supersaturated solid solution, and finally artificially aged (AA). Investigations were carried out to study the effect of welding, and artificial aging on microstructure, elongation, strength, and Vickers microhardness of TIG welded AA7075.

2 EXPERIMENTAL PROCEDURES

2.1. Materials

In the present study, AA7075-T6 sheets with 140*120 mm dimensions with a thickness of 1.5 mm were cut and prepared. Also, sub-size tensile test specimens were cut following the ASTM E08 standard [22] in the rolling direction using a wire cut machine. Uniaxial tensile tests were carried out on a SANTAM universal testing machine at a speed of 1 mm/min using an extensometer with a 50 mm gauge length to measure exact displacements. The 0.2% offset yield strength, ultimate tensile strength, and elongation at break were evaluated for tensile specimens. The Chemical composition of the base material in the as-received condition and filler rod are shown in “Table 1”. Vickers microhardness (HV) test was also performed using a Vickers indenter with 300gf load and 10s dwell time according to ASTM E384-16 standard [23].

Table 1 Chemical composition (wt. %) of base metal (AA 7075) and filler metal (5356)

Material	Zn	Mg	Cu	Cr	Fe	Si	Ti	Mn	Zr	Al
AA7075	5.70	2.02	1.35	0.18	0.15	0.07	0.047	0.02	0.01	Remaining
Filler metal (5356)	0.10	5.50	0.10	0.12	0.40	0.25	0.13	0.10	-	Remaining

2.2. Preheating

Preheating builds up additional heat which decreases the cooling rate of a welded joint. Preheating does not affect the final outlook of the weld zone cross-section but may improve the weld joint properties. The extra heat of preheating increases the temperature of the material around the weld zone to facilitate welding. In this work, AA7075 sheets were first cleaned and deoxidized with a wire brush and acetone solution. The sheets were then subjected to 80 ° C for a period of 4 minutes in a furnace to obtain a homogeneous microstructure throughout the sheets [24]. By preheating, the sheets are prepared for welding with a moderate thermal gradient.

2.3. Welding Operation

The GTAW process was selected for welding as this process produces high-quality welds [11] at a reasonable cost. One of the most critical factors to consider for GTAW is the filler metal. The ER5356 (Mg-rich) plays an important role in the strength of the weldment joint due to its good penetration depth [25]. The filler metal ER5356 of 1.6 mm diameter was therefore used for butt welding the sheets under the conditions given in “Table 2”.

Table 2 GTAW welding process parameters

Tungsten electrode diameter (mm)	2.4
Filler rod diameter (mm)	1.6
Alternating Current (AC) (A)	90-110
Welding speed (mm /min)	16
Gas flow rate (l /min)	10
Pre-heat temperature (◦C)	80
Shielding gas	Argon
Gas pressure (bar)	100
Gas purity	99.99 %

In this work, a thick plate with a V-shaped groove was used as a fixture to fix the sheets with a root gap of 1mm during the welding process as shown in “Fig. 1(a)”. Before welding, the parts and fixture surfaces were cleaned with a soft wire brush and acetone solution to remove oxides and other contaminants. The welding direction was chosen perpendicular to the sheet's rolling direction. GTAW welding process parameters were set according to “Table 2”. The welding process was performed manually as shown in “Fig. 1(a)”. Figure 1. (b) shows the welded blank with the designed set-up.

Welded samples were prepared for tensile, microhardness, and metallographic tests to evaluate the mechanical properties ("Fig. 2"). The specimens were prepared perpendicular to the weld line ("Fig. 2 (b)").

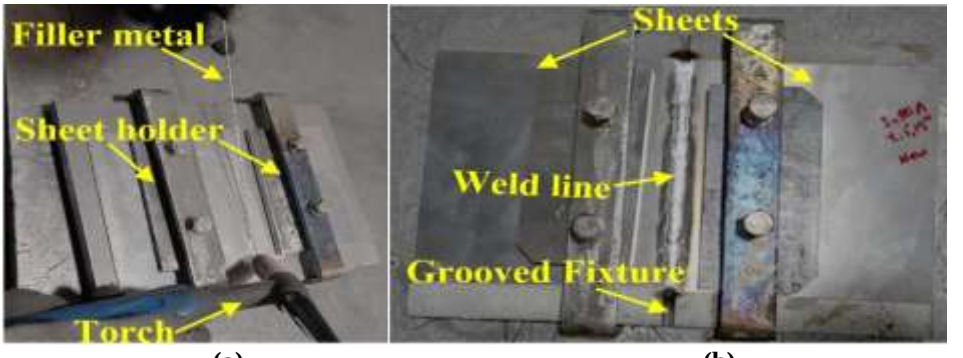

(a) **(b)**

Fig. 1 The welding set-up: (a): Fixture for welding the sheets, and (b): The final welded blank.

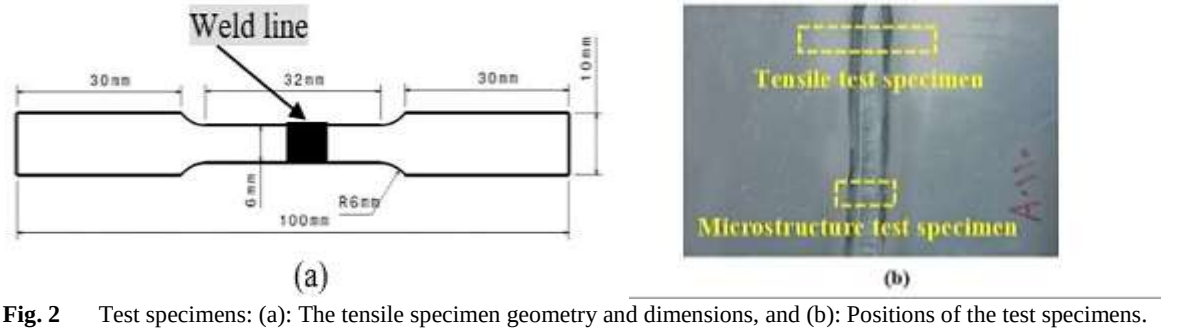

Fig. 2 Test specimens: (a): The tensile specimen geometry and dimensions, and (b): Positions of the test specimens.

2.4. Post-Weld Heat Treatment

For post-weld heat treatment of the welded blank, the solution heat treatment was first performed at 480 °C for a soaking time of 10 min using a controlled temperature furnace. The solution heat treated samples were then quenched to ambient temperature as quickly as possible using a flat water-cooling die. Finally, an artificial aging operation was carried out at 120°C for a soaking time of 24 h in a heat treatment furnace to complete the post-weld heat treatment.

2.5. Uniaxial Tensile and Hardness Tests

To obtain tensile properties (tensile strength σ_U, yield strength σ_Y, percentage of elongation El%, and fracture strength σ_F), uniaxial tensile tests with a constant strain rate of 1 mm/min were carried out. The tensile specimens for the welded blank (WB) and the AA specimen were prepared perpendicular to the welding direction using a wire cutting machine as explained in section 2.1, according to ASTM E8 [22].

Vickers microhardness (HV) test was also performed (as explained in section 2.1) to measure the hardness values of the BM, the WB, and the AA specimen. The hardness profiles were obtained over the joint cross-section using ASTM E384-16 standard [23].

2.6. Metallography

Metallographic samples were prepared as ASTM E3-11 standard [26] technique using sandpaper and alumina powder for polishing. After polishing, the etching solution of nitric acid, hydrochloric acid, hydrofluoric acid, and distilled water was first used and the final etching was done with a modified chlorine solution, according to ASTM E883-11 [27] to reveal the microstructure. The microstructural analysis was performed using an optical microscope. Also, An X-ray diffraction (XRD) test was performed to identify the phases in the as-received AA7075.

3 RESULTS AND DISCUSSION

3.1. Microstructure Studies

To describe the characteristics of the weldment joint, a cross-sectional macrograph of FZ, HAZ, and BM zones of WB is shown in "Fig. 3". Figur 4" shows that the microstructure morphology of the BM has a typical rolled structure, and the grains are banded or fibrous along the deformation direction. The base metal microstructure consisting of coarse and elongated Al grains with a dispersion of fine and coarse precipitates diffused in the field of α matrix of the alloy is shown in "Fig. 4".

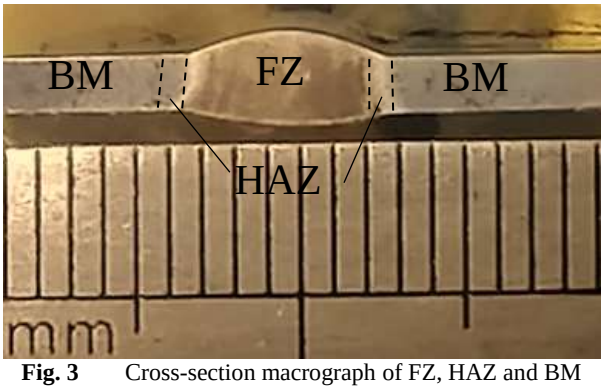

Fig. 3 Cross-section macrograph of FZ, HAZ and BM zones in the WB.

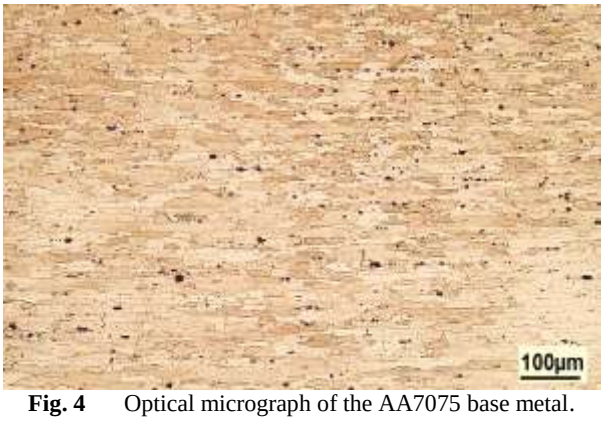

Fig. 4 Optical micrograph of the AA7075 base metal.

The XRD graph for the as-received AA7075 is shown in "Fig. 5".

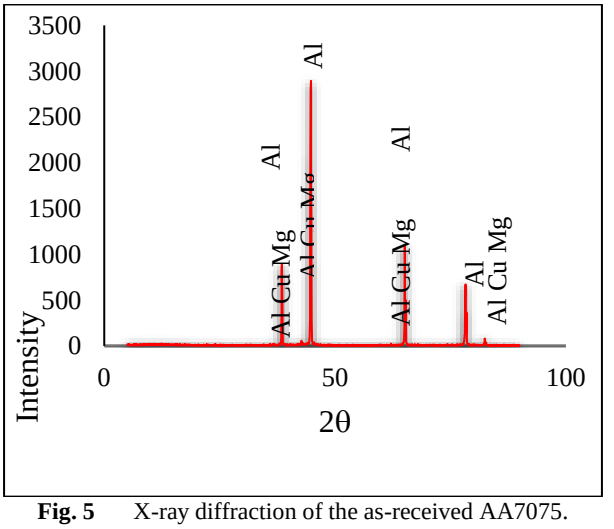

Fig. 5 X-ray diffraction of the as-received AA7075.

This XRD reveals the different contents of phase compositions of the alloy. Based on the peaks of the graph, it is observed that the microstructure consists of Al, AlCuMg, and Al_2CuMg particles. The very small precipitates of $MgZn_2$ also act as a strengthening phase of aluminum alloy 7075 as reported by other researchers [28-29]. However, the presence of $MgZn_2$ was not detected, which may be due to the XRD technique that was not sensitive enough to study the low content of $MgZn_2$ intermetallic phases or the dissolving of some Zn and Mg atoms in the Al matrix.

As observed in the optical micrograph of HAZ and FZ of the WB in "Fig. 6", the precipitates are dispersed inside the grains and at the grain boundaries. The overaging caused by the welding heat input that leads to the formation of coarse precipitates inside the FZ spherical grains reduces the strength and hardness. In contrast to the base metal's microstructure, the microstructure of the FZ consisted of equiaxed grains. The dispersion of precipitates into the matrix of the FZ is due to the incidence of dynamic recrystallization. The hardening phase dissolution operation in the matrix during the welding process and the increased grain size near the molten pool cause greater softening and a reduction in the mechanical properties of the HAZ as reported by Gomez et al. [20].

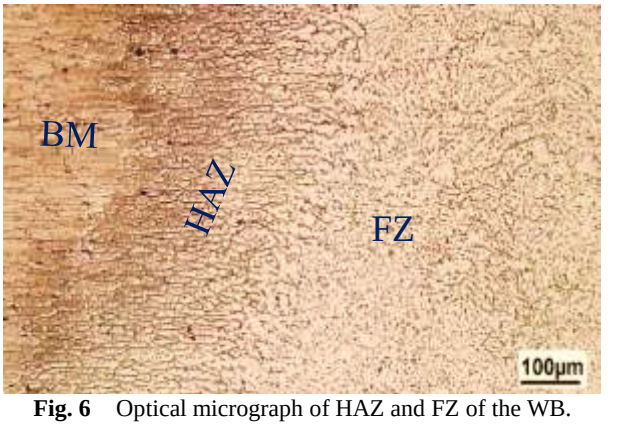

Fig. 6 Optical micrograph of HAZ and FZ of the WB.

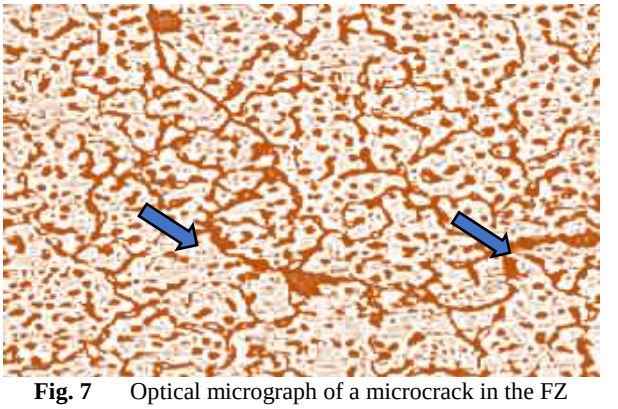

Fig. 7 Optical micrograph of a microcrack in the FZ (200X).

The properties of the FZ of the WB are also affected by the filler metal type. As mentioned earlier in the introduction section, welding with dissimilar filler metal ER5356 dilutes the melting zone and the concentration of the alloying elements of AA7075 decreases resulting

in a decrease in weld strength and an increase in the likelihood of liquation cracking [18-19]. This type of crack was observed in the FZ of the WB as shown in "Fig. 7". Microcracks of this nature usually originate from grain boundaries where intergranular cracks developed.

Figure 8 presents the microstructure of the BM of the WB after artificial aging (AA) at 120°C for 24 h. Artificial age hardening of the 7075-type alloys is considered the main source of alloy strength [28]. During the AA process, several structural transformations such as precipitation hardening, solid solution strengthening, and grain refinement occur within the aluminum alloy 7075.

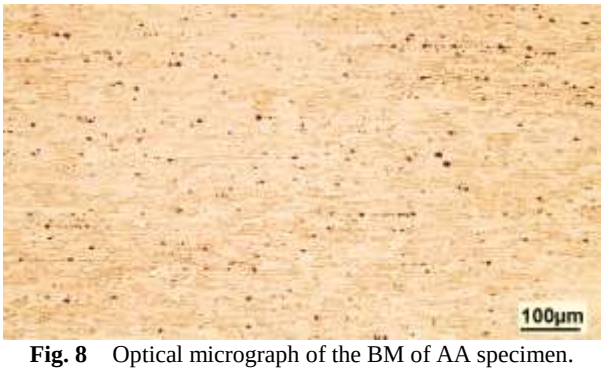

Fig. 8 Optical micrograph of the BM of AA specimen.

These mechanisms offer improved strength, hardness, and fatigue resistance. The fine precipitates within the microstructure of the alloy are composed of strengthening elements such as Cu, Zinc, and Mg. These precipitates act as obstacles to the movement of dislocations, leading to increased strength and hardness. The solid solutions formed during solid solution strengthening, and the fine-grain structures also contribute to better mechanical properties after the AA process. Comparison of micrographs of "Fig. 4" (initial material) and "Fig. 8" (AA specimen)" indicates the recovery of the microstructure and hence improvement in the mechanical properties after the AA operation. It is seen that after the AA process, the morphology of irregular coarse particles is changed into almost globular shapes, as also reported previously by Ding et al. [11].

Figure 9 reveals the changes and modification of the WB joint microstructure in three regions (BM, HAZ, and FZ) of the AA sample. Examining the microstructure of Fig. 9, the almost uniform distribution and fineness of precipitates in the HAZ matrix of the AA specimen due to proper aging operation tend to improve this zone's hardness and strength compared to those of the WB. After the aging process, the microstructure consisted of very fine and dense precipitates inside the grains, while precipitation density at the grain boundaries almost disappeared. The grain shape and morphology of FZ also showed the coaxial and regular grains. The smaller and more uniformly distributed precipitates inside the grains can lead to higher strength and hardness of the FZ of the AA sample.

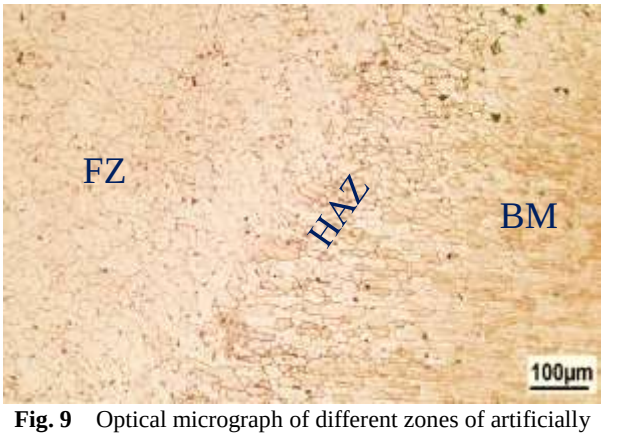

Fig. 9 Optical micrograph of different zones of artificially aged joint.

3.2. Tensile Properties

The tensile properties of the BM, the WB, and the AA specimens are presented in "Table 3" and "Fig. 10". The harmful effect of welding caused an almost 38% reduction in the tensile properties ($\boldsymbol{\sigma}_U$, $\boldsymbol{\sigma}_Y$, and $\boldsymbol{\sigma}_F$) of the WB compared to those of the BM. A 65% decrease in elongation was also observed. As stated earlier in section 3.1, these reductions are mainly due to the microstructural changes in the WB. However, post-weld heat treatment of the WB was found to be beneficial to enhance the tensile properties. Variations of mechanical properties indicate that the strength values of the AA specimen are very close to those of the BM. Despite a 65% loss of ductility of the WB, the aging operation caused improvements of 50% in elongation at break and 54% in fracture strength. Therefore, a noticeable improvement in mechanical properties can be achieved after proper post-weld heat treatment of the specimens.

Table 3 Mechanical properties ratios (%) of the BM, the WB, and the AA specimens

specimen	$\boldsymbol{\sigma_U}$ (MPa)	$\boldsymbol{\sigma_Y}$ (MPa)	$\boldsymbol{\sigma_F}$ (MPa)	El%
AA	546 (96 %)	445(90 %)	520 (100.4 %)	9 (69%)
WB	352 (62 %)	295 (60 %)	337 (65 %)	4.5 (35%)
AA7075	569 (100%)	495 (100%)	518 (100%)	13 (100%)

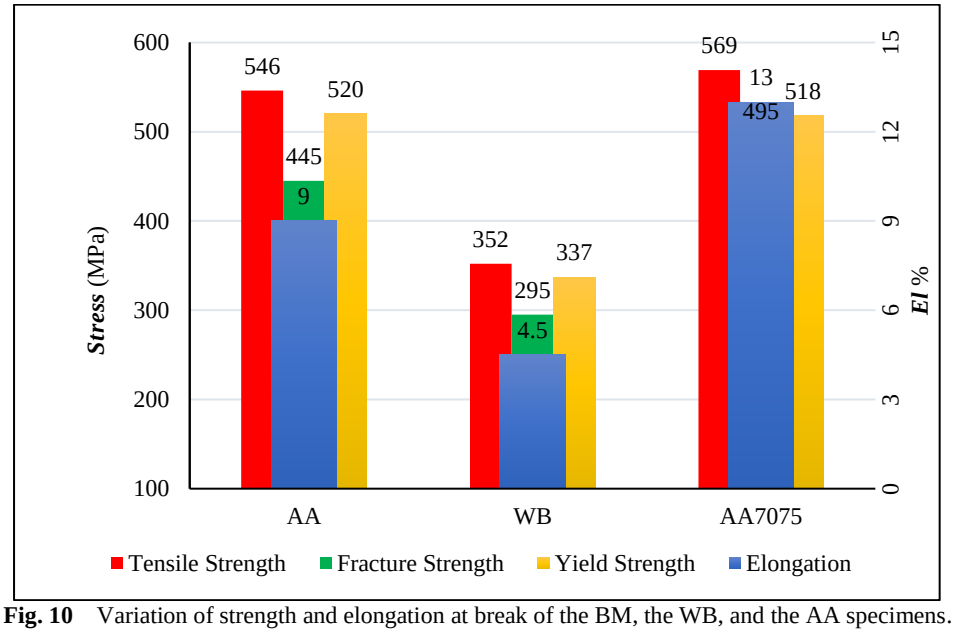

Fig. 10 Variation of strength and elongation at break of the BM, the WB, and the AA specimens.

3.3. Microhardness Measurement

The distribution of Vickers microhardness across the cross-section of the BM, the WB, and the AA specimens is presented in "Fig. 11". The detrimental effect of welding has resulted in the lowest hardness in the FZ and the HAZ of the WB, compared to those of the BM and the AA sample. The AA process performed on the WB caused an increase in the hardness level of different zones of the AA sample due to the mechanisms of precipitation hardening, solid solution strengthening, and grain refinement explained earlier. Figures 10 and 11 show that the fusion zones in the WB and the AA specimens have the lowest strength and hardness where the fracture occurs in the tensile test ("Fig. 12").

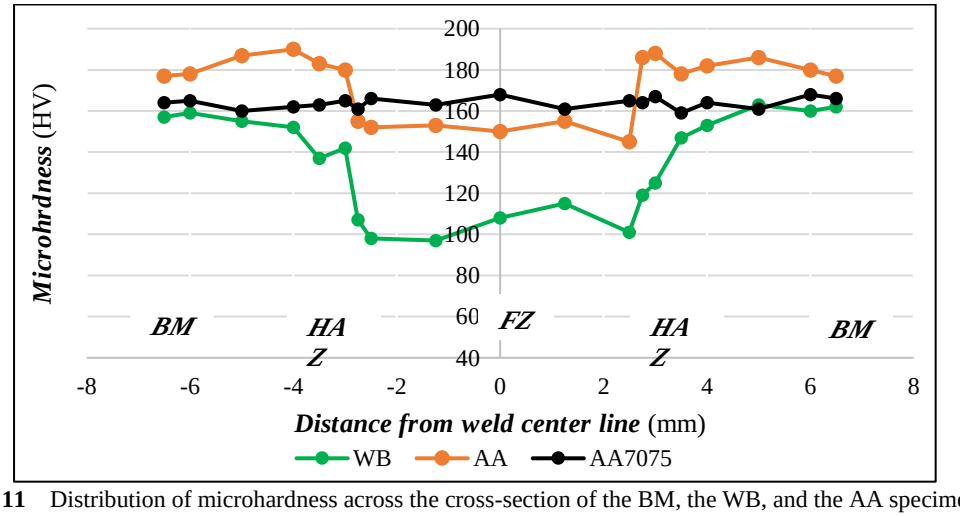

Fig. 11 Distribution of microhardness across the cross-section of the BM, the WB, and the AA specimens.

(a) (b)

Fig. 12 Fractures in the weld zone of: (a): The WB, and (b): The AA specimens.

4 CONCLUSIONS

In this article, 1.5 mm thick sheets of AA7075 were first preheated and welded using the gas tungsten arc welding process. The effect of post-weld heat treatment on the microstructure and mechanical properties of the welded parts was investigated. The results of this study demonstrate that:

1- The tensile properties and microhardness of the welded part decreased compared to those of the original sheet due to microstructural changes caused by welding.

2- The lowest Vickers microhardness of about 110 was observed in the fusion zone of the welded part compared to 170 of the base metal.

3- Welding caused an almost 40% reduction in yield, tensile, and fracture strengths and a 65% decrease in elongation.

4- The post-weld heat treatment performed on the welded part changed the microstructure and significantly improved the mechanical properties in such a way that the tensile properties and microhardness of the aged specimen were close to those of the base metal.

5- Tensile tests caused fractures in the fusion zones (weakest zone) of both the welded part and the artificially aged specimens.

REFERENCES

[1] Zheng, K., Politis, D. J., Wang, L., and Lin, J., A Review on Forming Techniques for Manufacturing Lightweight Complex-Shaped aluminum Panel Components, International Journal of Lightweight Materials and Manufacture, Vol. 1, No. 2, 2018, pp. 55-8. https://linkinghub.elsevier.com/retrieve/pii/S258884041830012X.

[2] Peter, I., Rosso, M., Study of 7075 Aluminum Alloy Joints, Scientific Bulletin of 'Valahia' University, Materials & Mechanics, Vol. 15, No. 13, 2017, pp. 7-11, Doi 10.1515/bsmm-2017-0011.

[3] Yildirim, M., Özyürek, D., and Gürü, M., The Effects of Precipitate Size on the Hardness and Wear Behaviors of Aged 7075 Aluminum Alloys Produced by Powder Metallurgy Route, Arabian Journal for Science and Engineering, Vol. 15, No. 41, 2016, pp. 4273–4281.

[4] Chen, R., Iwabuchi, A., and Shimizu, T., The Effect of a T6 Heat Treatment on The Fretting Wear of a Sic Particle-Reinforced A356 Aluminum Alloy Matrix Composite, Wear, Vol. 238, No. 2, 2000, pp. 110–119, DOI:10.1016/S0043-1648(99)00328-2.

[5] Li, Z., Xiong, B., Zhang, Y., Zhu, B., Wang, F., and Liu, H., Investigation of Microstructural Evolution and Mechanical Properties During Two-Step Aging Treatment at 115 and 160 ◦C in an Al–Zn–Mg–Cu Alloy Pre-Stretched Thick Plate, Materials Characterization, Vol. 59, No. 3, 2008, pp. 278–282, https://doi.org/10.1016/j.matchar.2007.01.006.

[6] Isadere, A. D., Aremo, B., Adeoye, M. O., Olawale, O. J., and Shittu, M. D., Effect of Heat Treatment on Some Mechanical Properties of 7075 aluminum Alloy, Materials Research, Vol. 16, No. 1, 2013, pp. 190–194, https://doi.org/10.1590/S1516-14392012005000167.

[7] Fakioglu, A., Özyürek, D., Effects of Re-Aging on the Fatigue Properties of aluminum Alloy AA7075, Materials Testing, Vol. 56, No. 7–8, 2014, pp. 575–582, https://doi.org/10.3139/120.110598.

[8] Wang, Z., Wang, S., Zhang, C., and Wang, Z., Effect of Post-Weld Heat Treatment on Microstructure and Mechanical Properties of 7055 Aluminum Alloy Electron Beam Welded Joint, Material Research Express, Vol. 7, 2020, 066528, https://doi.org/10.1088/2053-1591/ab9cea.

[9] Xu, D. K., Rometsch P. A., and Birbilis, N., Improved Solution Treatment for an As-Rolled Al−Zn−Mg−Cu Alloy, Part I. Characterisation of Constituent Particles and Overheating, Materials Science and Engineering A, Vol. 534, No. 2, 2012, pp. 234−243, https://doi.org/10.1016/j.msea.2011.11.065.

[10] Liu, J., Li, H., Li, D., and Yue, W., Application of Novel Physical Picture Based on Artificial Neural Networks to Predict Microstructure Evolution of Al−Zn−Mg−Cu Alloy During the Solid Solution Process, Transactions of Nonferrous Metals Society of China, Vol. 25, No. 3, 2015, pp. 944−953, https://doi.org/10.1016/S1003-6326(15)63683-4.

[11] Ding, J., Wang, D., Wang, Y., and Du, H., Effect of Post Weld Heat Treatment on Properties of Variable Polarity TIG Welded AA2219 Aluminium Alloy Joints, Transactions of Nonferrous Metals Society of China, Vol. 24, No. 5, 2014, pp. 1307-1316, doi.org/10.1016/S1003-6326(14)63193-9.

[12] Asadi, P., Alimohammadi, S., Kohantorabi, O., Soleymani, A., and Fazli, A., Numerical Investigation on The Effect of Welding Speed And Heat Input on The Residual Stress of Multi-Pass TIG Welded Stainless Steel Pipe, Proceedings of the Institution of Mechanical Engineers, Part B: Journal of Engineering Manufacture, 2021, Vol. 235, No. 6-7, pp. 1007–1021, doi.org/10.1177/0954405420981335.

[13] Asadi, P., Alimohammadi, S., Kohantorabi, O., Fazli, A., and Akbari, M., Effects of Material Type, Preheating and Weld Liang, Improving Mechanical Properties of PVPPA Welded Joints of 7075 Aluminum Alloy by PWHT, Materials, Vol. 11, No. 3, 2018, pp. 379, https://doi.org/10.3390/ma11030379.

[14] Miles, M. P., Decker, B. J., and Nelson, T. W., Formability and Strength of Friction stir-welded

Aluminum Sheets, Metallurgical and Materials Transactions A, Vol.35, 2004, pp. 3461–3468.

[15] Xiao, L., Chenyang, W., Xiaoping, L., Bin, Z., and Runzhou, L., Investigation of 7075 Aluminum Alloy TIG Welding Joint Using 7075 Aluminum Alloy Wire Before and After Heat Treatment, Materials Research Express, Vol. 10, No. 4, 2023, https://doi.org/10.1088/2053-1591/accac4.

[16] Tušek, J., Klobčar, D., Tungsten inert gas (TIG) welding of aluminum alloy EN AW-AlZn5.5MgCu, Metalurgija Vol. 55, No. 4, 2016, pp. 737–40.

[17] Sokoluk, M., Cao, C., Pan, S., and Li, X., Nanoparticle-Enabled Phase Control for Arc Welding of Unweldable Aluminum Alloy 7075, Nature Communications, Vol. 10, 2019, pp. 98, https://doi.org/10.1038/s41467-018-07989-y.

[18] Kou, S., Solidification and Liquation Cracking Issues in Welding, Vol. 55, No. 6, 2003, pp. 37–42, http://dx.doi.org/10.1007/s11837-003-0137-4.

[19] Gomez, J. M., Salazar, D. E., Urena, A., Villauriz, E., Manzanedo, S., and Barrenaa, I., TIG, and MIG Welding of 6061 and 7020 aluminum Alloys, Microstructural Studies and Mechanical Properties, Welding International, Vol. 13, No. 4, 2010, pp. 293-295, https://doi.org/10.1080/09507119909447381.

[20] Janaki Ram, G. D., Mitra, T. K., Shankar, V., and Sundaresan, S., Microstructural Refinement Through Inoculation of Type 7020 Al–Zn–Mg Alloy Welds and Its Effects on Hot Cracking and Tensile Property, Journal of Materials Processing Technology, Vol. 142, No. 1, 2003, pp. 174–81, https://doi.org/10.1016/S0924-0136(03)00574-0.

[21] E28 Committee, Test Methods for Tension Testing of Metallic Materials, ASTM International, DOI: 10.1520/E0008_E0008M-13A.

[22] E04 Committee, Standard Test Method for Microindentation Hardness of Materials, ASTM International, DOI: 10.1520/E0384-16.

[23] Yeni, C., Sayer, S., Pakdil, M., Comparison of Mechanical and Microstructural Behavior of TIG, MIG, and Friction Stir Welded 7075 Aluminum Alloy, Vol. 47, No. 5, 2009, pp. 341–347.

[24] Mabuwa, S., Msomi, V., Review on Friction Stir Processed TIG and Friction Stir Welded Dissimilar Alloy Joints, Metals, Vol. 10, No. 1, 2020, pp. 142, doi:10.3390/met10010142.

[25] E04 Committee, Standard Guide for Preparation of Metallographic Specimens, E3–11. DOI:10.1520/E0003-11R17.

[26] E04 Committee, Standard Guide for Reflected–Light Photomicrography, E883 – 11. DOI: 10.1520/E0883-11R17.

[27] Tahmasbi, A., Samuel, A. M., Zedan, Y., Songmene, V., and Samuel, F. H., Effect of Aging Treatment on the Strength and Microstructure of 7075-Based Alloys Containing 2% Li and/or 0.12% Sc, Materials, Vol. 16, No. 23, 2023, pp. 7375, https://doi.org/10.3390/ma16237375.

[28] Ghosh, A., Ghosh, M., Microstructure and Texture Development of 7075 Alloy During Homogenization, Philoso Phical Magazine, 2018, https://doi.org/10.1080/14786435.2018.1439596.

[29] Li, G., Chen, F., and Han, Y., Pass Number on Residual Stress of Welded Steel Pipes by Multi-Pass TIG Welding (C-Mn, SUS304, SUS316), Asadi, Thermal Science and Engineering Progress, Vol. 16, 2020, 100462, https://doi.org/10.1016/j.tsep.2019.100462.